ADVANCING EARTH AND SPACE SCIENCE

Geophysical Research Letters

RESEARCH LETTER

10.1029/2020GL092321

Key Points:

- Monsoons are due to a non-additive response to three forcings: land-sea contrast, orography, and ocean heat transport
- The non-additivity in precipitation leads to a non-additive response of the upper level stationary waves and Asian monsoon anticyclone
- Gross moist stability can account for this effect, but not the land-sea breeze paradigm

Supporting Information:

Supporting Information may be found in the online version of this article.

Correspondence to:

C. I. Garfinkel,
chaim.garfinkel@mail.huji.ac.il

Citation:

Garfinkel, C. I., White, I. P., Gerber, E. P., Adam, O., & Jucker, M. (2021). Nonlinear interaction between the drivers of the monsoon and summertime stationary waves. *Geophysical Research Letters*, *48*, e2020GL092321. https://doi.org/10.1029/2020GL092321

Received 5 JAN 2021
Accepted 1 JUN 2021

Nonlinear Interaction Between the Drivers of the Monsoon and Summertime Stationary Waves

Chaim I. Garfinkel[1], Ian P. White[1], Edwin P. Gerber[2], Ori Adam[1], and Martin Jucker[3]

[1]Fredy and Nadine Herrmann Institute of Earth Sciences, Hebrew University, Jerusalem, Israel, [2]Courant Institute of Mathematical Sciences, New York University, New York, NY, USA, [3]Climate Change Research Center and ARC Centre of Excellence for Climate Extremes, University of New South Wales, Sydney, NSW, Australia

Abstract A moist General Circulation Model is used to investigate the forcing of the Asian monsoon and the associated upper level anticyclone by land-sea contrast, net horizontal oceanic heat transport, and topography. The monsoonal pattern is not simply the linear additive sum of the response to each forcing; only when all three forcings are included simultaneously does the monsoonal circulation extend westward to India. This nonadditivity impacts the location of the upper level anticyclone, which is shifted eastward and weaker if the forcings are imposed individually. Sahelian precipitation, and also austral summer precipitation over Australia, southern Africa, and South America, are likewise stronger if all forcings are imposed simultaneously. The source of the nonlinearity can be diagnosed using gross moist stability, but appears inconsistent with the land-sea breeze paradigm. This non-additivity implies that the question of which forcing is most important may be ill-posed in many regions.

Plain Language Summary Monsoons dominate the climate in many regions of the tropics and subtropics, and are characterized by rainy summer and drier winter seasons. This rainfall is crucial for agriculture, among other societal implications, in heavily populated regions of the world. The processes leading to regional confinement of the monsoons are investigated using an intermediate complexity moist General Circulation Model. We find that a linear perspective cannot account for the monsoons; only when land-sea contrast, orography, and ocean heat transport are included simultaneously does the monsoonal circulation extend westward to India. A similar nonlinearity is evident for Sahelian precipitation, and also for austral summer precipitation over Australia, southern Africa, and South America.

1. Introduction

Monsoons dominate the climate in many regions of the tropics and subtropics, and are characterized by rainy summers. This rainfall is crucial for agriculture, among other societal implications, in heavily populated regions of the world. The monsoons are also a critical component of the large scale stationary wave pattern in summertime, and through the associated upper level anticyclone over Asia it regulates transport into the stratosphere (Gill, 1980; Randel & Park, 2006; Rodwell & Hoskins, 1996; Vernier et al., 2015).

Traditionally, the localization of summertime rainfall near land led to the interpretation of monsoons as a large-scale sea-breeze, with moist air drawn over the warmer continent from the neighboring ocean, leading to convective rainfall over land (Halley, 1687), with a subsequent large-scale circulation driven by convective heating (Gill, 1980). This interpretation of monsoons as a sea breeze is seemingly contradicted by a few facts: land-sea temperature contrast peaks prior to monsoon onset over South Asia (Simpson, 1921) (though the tropospheric thermal contrast and monsoonal rainfall seasonalities do coincide), and interannual variability in land surface temperatures and total monsoonal precipitation are negatively correlated (Kothawale & Kumar, 2002). More recent perspectives of monsoons view them as part of a "global monsoon mode" in which the tropical convergence zone migrates seasonally (Geen et al., in press; Trenberth et al., 2000; B. Wang et al., 2009; P. X. Wang et al., 2017), with regional monsoons as localized and more extreme migrations due to a favorably positioned and low heat-capacity continent (Gadgil, 2018) and due to orography, for example, over Asia (Acosta & Huber, 2020; Chiang et al., 2020; Li & Yanai, 1996). In this view, a peak in near-surface moist static energy or equivalent potential temperature can accurately diagnose the seasonality and interannual variability in monsoonal precipitation

(Eltahir & Gong, 1996; Hurley & Boos, 2013; Ma et al., 2019) and more generally tropical convergence zones are located where differences in the moist static energy between the upper and lower troposphere are small (Neelin & Held, 1987).

While both orography and land-sea contrast (hereafter LSC) have been recognized as crucial for monsoons (see the discussion in Xu et al., 2009), the relative importance of LSC and orography in forcing monsoons is less clear. Xu et al. (2009) find that zonal LSC and orography are of similar importance in determining the extent of Asian monsoon, though the meridional land-sea thermal contrast is relatively unimportant. However Xu et al. (2009) do not consider the possible nonlinear interactions between these building blocks (rather they incrementally make the model more realistic), and as shown in Garfinkel et al. (2020a), nonlinear interactions can be large in other seasons.

Several studies have aimed to delineate the fundamental dynamics of the monsoon using simplified models of the atmosphere, as this allows for isolating the relevant factors controlling the structure of tropical precipitation and stationary waves. Specifically, dry models with imposed convective-like diabatic heating have shown that the large scale stationary wave pattern in summer is dictated in a generally linear manner as the sum of the responses to the heating and to orography (Hoskins & Rodwell, 1995; Rodwell & Hoskins, 1995, 1996, 2001), with diabatic heating playing the dominant role and orography mainly affecting the regional details. However such models must pre-determine the heating profile, which precludes nonlinear interactions between LSC and orography in determining the structure and magnitude of the heating and thus may underestimate the degree of nonlinearity (as discussed in Garfinkel et al., 2020a).

Moist models do not need to pre-specify the pattern and magnitude of the heating, and experiments using moist models with idealized continents have proven helpful in isolating the impact of specific forcings (e.g., Bordoni & Schneider, 2008; Geen et al., 2018, 2019; Maroon et al., 2016; Privé & Plumb, 2007; Shaw, 2014; Zhou & Xie, 2018). The results from these studies bolster the view of monsoons as a local manifestation of the global tropical convergence zone. However, the relevance of the monsoon in these idealized models to Earth's monsoons remains unclear, as they generally cannot simulate the full meridional and zonal structure of observed monsoons.

Other studies have used more comprehensive models with full physics to identify the impact of orography in a given region (Baldwin et al., 2019; Boos & Kuang, 2010; Chen & Bordoni, 2014; Wei & Bordoni, 2016; Wu et al., 2012; Xu et al., 2010), or to force surface temperature over continents to be similar to that of neighboring oceans (Chao & Chen, 2001), and then explore how monsoon strength and location changes. These comprehensive models, however, tend to be less flexible and are tuned such that removing too many relevant forcings leads to unstable behavior. A model that can fully bridge between comprehensive and moist aquaplanet models has, until very recently, been lacking, though the full configuration of Geen et al. (2018) was an important step forward.

While the aforementioned studies have made significant progress toward uncovering the building blocks of monsoons, there are still several open questions that we address in this study:

1. Can one reconstruct the full magnitude of monsoons by adding the individual building blocks, that is, LSC, topography, and ocean heat transport (hereafter OHT), to an aquaplanet model with initially no zonally asymmetric bottom forcings?
2. To what extent do the various building blocks of monsoons interact nonlinearly with each other?
3. How does the degree of nonlinearity change regionally, for example between the South Asian (i.e., Indian subcontinent) and East Asian monsoons?
4. To the extent that nonlinearities exist, can we provide a diagnostic budget for the emergence of these nonlinearities?

The rest of this paper introduces a model capable of answering these four questions (Section 2), answers them (Section 3), and then considers the implications for the summertime stationary waves (Section 4).

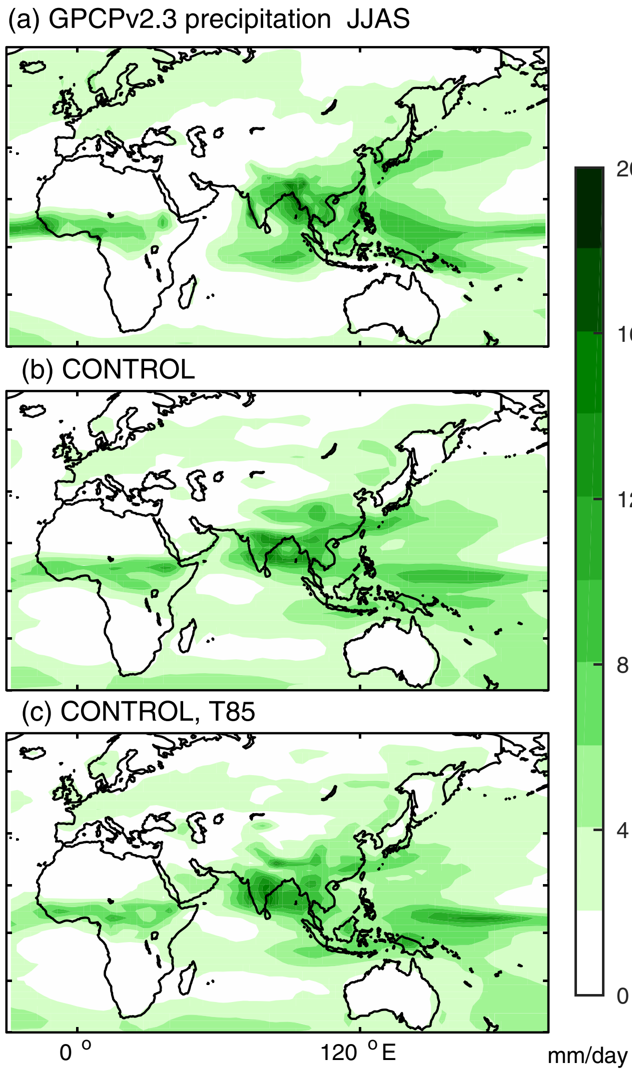

Figure 1. Precipation in June through September (a) in GPCPv2.3, (b) in the CONTROL integration with T42 resolution, and in (c) the CONTROL integration with double the horizontal resolution (T85). The contour interval is 2 mm/day.

2. The Monsoon in a Model of an Idealized Moist Atmosphere (MiMA), Version 2

In order to answer the questions posed in the previous section, we use the model of an idealized moist atmosphere (MiMA) introduced by Jucker and Gerber (2017), Garfinkel et al. (2020a), and Garfinkel et al. (2020b). This model builds on the aquaplanet model of Frierson et al. (2006), Frierson et al. (2007), and Merlis et al. (2013). Very briefly, the model solves the moist primitive equations on the sphere, employing a simplified Betts-Miller convection scheme (Betts, 1986; Betts & Miller, 1986), idealized boundary layer scheme based on Monin-Obukhov similarity theory, a purely thermodynamic, or slab, ocean, and the Rapid Radiative Transfer Model (RRTMG) radiation scheme (Iacono et al., 2000; Mlawer et al., 1997). Please see Jucker and Gerber (2017) for more details.

Three sources of zonal asymmetry are added to the lower boundary of an initially zonally symmetric moist aquaplanet model: orography, prescribed east-west OHT, and LSC (i.e., difference in heat capacity, surface friction, and moisture availability between oceans and continents). The specification of these forcings is identical to that in Garfinkel et al. (2020b), and is not repeated for brevity. This default model configuration is referred to as CONTROL for the rest of this paper. Integrations with all possible combinations of these three forcings have been created (in contrast to Xu et al. [2009]), including an integration with no zonally asymmetric surface forcings (hereafter no-forcing), and these integrations are summarized in Table S1. Note that all integrations (including the no-forcing integration) still include north-south OHT (Equation A4 of Garfinkel et al., 2020b). For reference, a detailed comparison between our model and the *full* configuration of Geen et al. (2018) is provided in the supplemental material.

The model is forced with CO_2 concentrations fixed at 390ppmv, and seasonally varying solar insolation. Unless otherwise indicated, all simulations in this paper were run with a triangular truncation at wavenumber 42 (T42) with 40 vertical levels for 38 years after discarding at least 10 years as spinup. The aim of this study is not to determine which specific orographic feature(s) is most important for the monsoon (as done by Boos & Kuang, 2010, among other). Here we either include all orographic features as resolved by the model at T42 resolution, or none.

The resulting climatological precipitation in June through September (JJAS) in CONTROL is shown in Figures 1b and 1c, and observed precipitation sourced from the Global Precipitation Climatology Project (GPCP) version 2.3 is shown in Figure 1a. (The precipitation in each experiment in Table S1 is shown in Figure S1). Precipitation over South and East Asia is of similar magnitude to that observed (Figure 1a), and largely occurs in the correct location, on large-scales. The climatological stationary waves in CONTROL and in the ERA-5 reanalysis (Hersbach et al., 2020) in 200 hPa geopotential height and streamfunction are shown in Figures S2 and S3. CONTROL captures the upper-level anticyclone above the monsoon in essentially the correct location and with a reasonable magnitude. While some of the fine-scale structure of precipitation and the stationary waves is not captured, our focus in this paper will be on larger scale differences (e.g., between South and East Asia). While not perfect, we consider our model a useful tool to understand how orography, OHT, and LSC interact to form the monsoon.

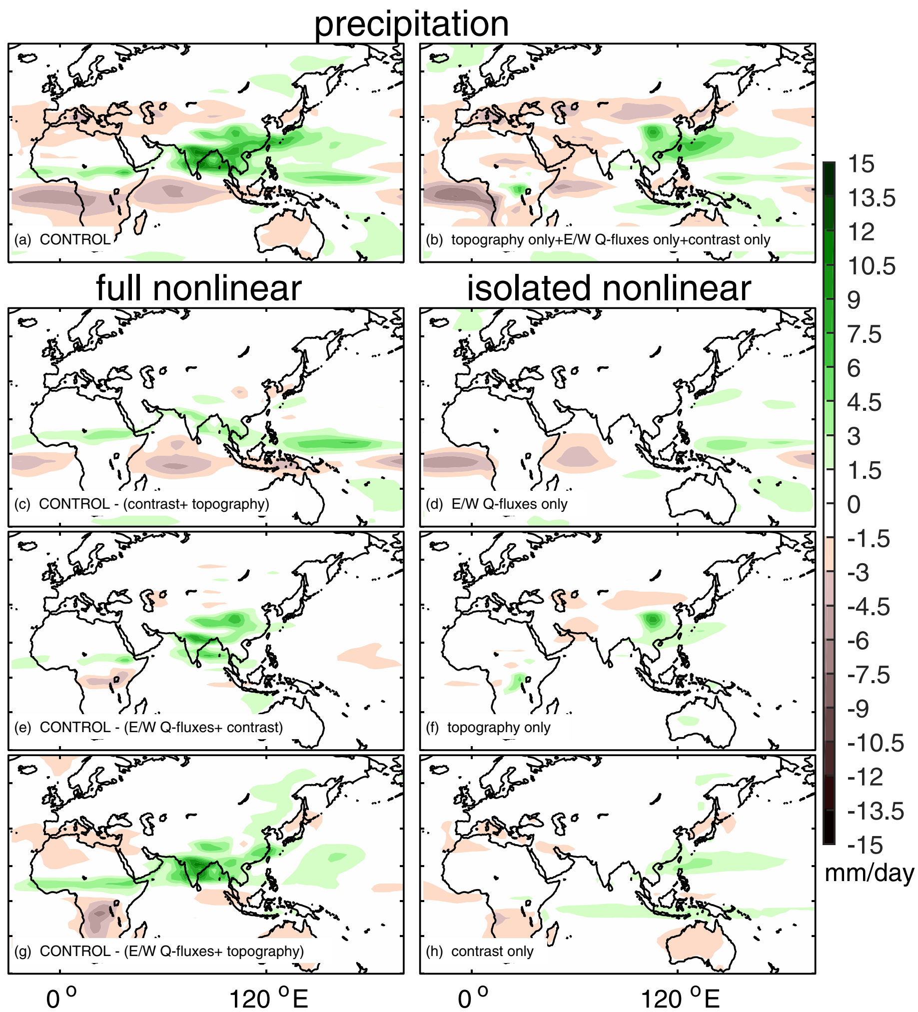

Figure 2. Precipitation in June-September (a) in CONTROL as compared to no-forcing, (b) as in (a) but for the sum of integrations with topography only, land-sea contrast (LSC) only, and ocean heat transport (OHT) only as compared to no-forcing; (c) the difference between CONTROL and the integration with LSC and topography; (d) integration with only OHT as compared to no-forcing; (e) the difference between CONTROL and the integration with OHT and LSC; (f) integration with only topography as compared to no-forcing; (g) the difference between CONTROL and the integration with OHT and topography; (h) integration with only LSC as compared to no-forcing. The contour interval is 1.5 mm/day.

3. Non-Additivity of the Monsoon

We first consider whether the monsoon can be decomposed linearly into the response to the various forcings. Figure 2a shows the difference in precipitation between CONTROL and no-forcing (exp 0 on Table S1). For Figure 2b, we first calculate the responses when each of the forcings is added separately to no-forcing, that is, the difference between topography only and no-forcing, OHT only and no-forcing, and LSC only and no-forcing. We then sum the precipitation response in these three individual forcing experiments. The net effect is that Figure 2b shows the precipitation response to the three forcings when the response to each forcing is computed in isolation. While the precipitation over East Asia in CONTROL appears to be associated with the linear summation of the forcings, the precipitation over India and the Sahel is much stronger when the forcings interact (Figure 2a vs. Figure 2b).

Which forcings are most responsible for the non-additive behavior? Before proceeding we review the definition of the isolated and full nonlinear response of Held et al. (2002). Taking OHT as an example, the isolated nonlinear response to OHT occurs when OHT is compared to no-forcings, while the full nonlinear response

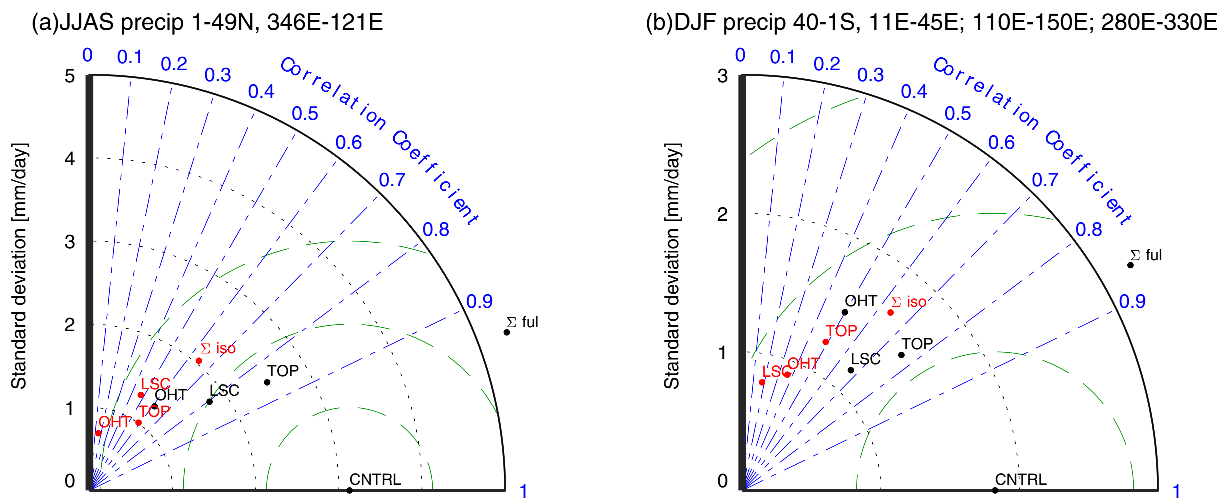

Figure 3. Taylor diagram of the precipitation response to each forcing, using the difference between CONTROL and no-forcing as the reference. The (red) isolated and (black) full nonlinear response to topography, land-sea contrast, and oceanic heat transport, as well as the sum of the isolated nonlinear (iso) and sum of the full nonlinear responses (ful), are shown. (a) Northern Hemisphere from 1 to 49°N and 346 to 121°E; (b) in December through February from 1 to 40°S and 11 to 45°E (Africa), 110–150°E (Australia), and 280–330°E (South America). Isolines of the centered root mean square difference equal to 1, 2, and 3 mm/day are shown in green.

to OHT occurs when OHT is added to a configuration that already has the other two forcings (or is the first to be removed from CONTROL).

The bottom three rows of Figure 2 show the precipitation response to each forcing imposed in isolation (right column; isolated nonlinear response) and also when each forcing is removed from CONTROL (left column; the full nonlinear response). For example, Figure 2c considers the difference in precipitation between CONTROL and the experiment where both LSC and topography are imposed but OHT is not. Hence, the precipitation response in Figure 2c is that forced by OHT when imposed on a basic state that already includes LSC and topography (the full nonlinear response). This pattern in Figure 2c can be compared to the isolated nonlinear response to OHT in Figure 2d. OHT in isolation has a limited impact on the precipitation in monsoonal regions, but if imposed on the basic state set up by topography and LSC, OHT leads to a strengthened monsoon over South and East Asia and enhanced precipitation over the Sahel.

Figure 2e shows the full nonlinear response to topography, while Figure 2f shows the isolated nonlinear response to topography. Precipitation is limited to East Asia in the isolated nonlinear response, but extends over India in the full nonlinear response. Figure 2g shows the full nonlinear response to LSC, while Figure 2h shows the isolated nonlinear response. The isolated nonlinear response is weaker than the full nonlinear response in all monsoonal regions, with the differences particularly pronounced over South Asia: there is no Indian monsoon in the isolated nonlinear response. Similar non-additivity is evident if we consider omega at 500 hPa (Figure S4) instead of precipitation: the response to each forcing, and especially to LSC, depends on the background state on which it is imposed.

Due to the strong non-additivity, one must be cautious in ranking the relative importance of the factors as the forcings interact. However there is a general indication that topography and LSC are more important over South and East Asia than OHT, while all three are important over the Sahel. The overall importance of each factor can be succinctly summarized in the Taylor diagram (Taylor, 2001) in Figure 3a. The reference state for the Taylor diagram is the difference between CONTROL and no forcing in Figure 2a, to which we then compare the isolated and full nonlinear responses to each forcing and also the sum of the isolated nonlinear and the sum of the full nonlinear responses. The full nonlinear responses to each forcing are closer to the total response than the accompanying isolated nonlinear responses, and topography (TOP) and LSC are more important that OHT.

In order to understand these nonlinearities, we consider the gross moist stability (GMS; Neelin & Held, 1987; Raymond et al., 2009) of the atmosphere. The uses of GMS are discussed in detail in Neelin and Held (1987)

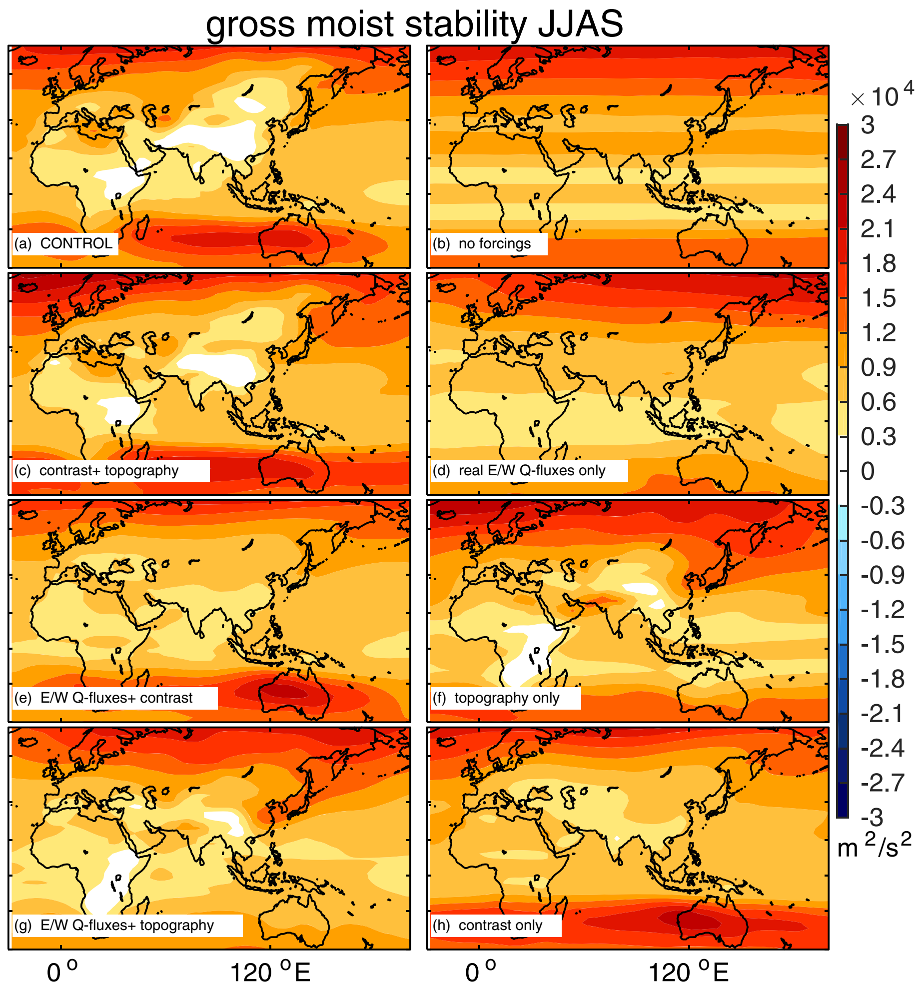

Figure 4. Mean state gross moist stability (defined as the difference in moist static energy between 250 hPa and 850 hPa) in June through September for the simulation with (a) CONTROL; (b) no forcings; (c) with land-sea contrast (LSC) and topography; (d) ocean heat transport (OHT) only; (e) OHT and LSC; (f) topography only; (g) OHT and topography; (h) LSC only.

and Raymond et al. (2009), but briefly, convection is expected to be located in regions with small (but positive) GMS, with dry conditions expected in regions with relatively high GMS. Furthermore, the strength of the convective response to a given external perturbation at the surface is inversely proportional to the GMS; that is, an energy flux into the atmosphere will have a stronger response if located in a region with smaller GMS.

Neelin and Held (1987) quantify GMS as the difference between the vertically integrated moist static energy above versus below the mid-troposphere, with the weight assigned to each level proportional to the divergence at that level (Equation 2.6 of Neelin & Held, 1987). Here we use a simplified version of this metric: the difference in moist static energy at 250 hPa versus 850 hPa, the two levels chosen to represent the upper and lower troposphere. The results are similar though noisier if we use the original definition, and are also similar if we choose levels adjacent to 250 hPa and 850 hPa. GMS in CONTROL is generally low in regions with strong monsoonal precipitation (Figure 4a) as expected.

Why are there nonlinearities in the response of the monsoon to these forcings? We first focus on why the response to OHT is stronger if imposed on a basic state that includes the other forcings (Figures 2c and 2d). The GMS for the integration with no forcings is shown in Figure 4b, while the GMS for the integration with LSC and topography included is shown in Figure 4c. GMS is clearly lower over South and East Asia in Figure 4c than in Figure 4b, and thus can explain the non-additive response. That is, the reduced GMS over Asia makes the atmosphere more sensitive to perturbations, amplifying the impact of OHT on the monsoons. Therefore, the response is larger in Figure 2c than in Figure 2d. The GMS is also lower over the Sahel and East Africa in Figure 4c than in Figure 4b, and thus can account for the non-additive behavior in precipitation in this region too.

GMS can also explain the stronger response to topography if imposed on a background state that already includes OHT and LSC. The GMS for the integration with OHT and LSC is shown in Figure 4e. GMS is lower over South and East Asia and Africa in Figure 4e than in Figure 4b, and thus the response to topography is stronger in Figure 2e than in Figure 2f. Finally, the GMS is lower over South and East Asia in the integration with OHT and topography than in no forcing (Figure 4g vs. Figure 4b), explaining the stronger response to the LSC in Figure 2g than in Figure 2h. While the focus of this paper is on boreal summer monsoons, December-February precipitation over South America, southern Africa, and Australia is stronger if the forcings are imposed on a basic state that already includes the other forcings (Figure 3b), and this effect is consistent with GMS (not shown).

Of the three forcings, OHT is least important for changes in GMS over South and East Asia. This can be inferred by comparing GMS in CONTROL (Figure 4a) with GMS in the integration with topography and LSC (Figure 4c), and also by noting that of the three individual forcing simulations in Figures 4d, 4f and 4h, the OHT integration (Figure 4d) is most similar to the no-forcing integration (Figure 4b). Over Africa, topography is most important for East Africa, while OHT is more important further west.

Overall, the individual building blocks of monsoons interact non-additively, such that the sum of the responses to each building block does not equal the response when all are imposed simultaneously. Gross moist stability can provide an explanation for this non-additivity. Nonlinear effects are particularly pronounced over South Asia and weaker over East Asia.

4. Impact on NH Summer Stationary Waves

The non-additivity observed in Section 3 for precipitation has implications for the upper-level anticyclone. It is well established that the upper-level anticyclone is driven by convection (Gill, 1980; Randel & Park, 2006; Rodwell & Hoskins, 2001), and hence it is reasonable to suspect a non-additive response to the building blocks of the anticyclone similar to that seen for precipitation. This expectation is confirmed in Figure 5, which mirrors Figure 2 but for 200 hPa streamfunction. Figures 5a and 5b compare stationary waves in CONTROL to the sum of the stationary wave pattern in the topography only, OHT only, and LSC only experiments. Consistent with the weakness of the precipitation over India and the Sahel in Figure 2b, the ridge over south Asia is shifted south in Figures 5b and 5a, and a trough is evident over the Northern Sahara. Similar figures for streamfunction at 850 hPa, height at 200 hPa, and zonal wind at 200 hPa (Figures S5, S6, and S7) also indicate a non-additive response.

The bottom three rows of Figure 5 show the response to each forcing imposed in isolation (right column; isolated nonlinear response) and also when each forcing is removed from CONTROL (left column; the full nonlinear response). OHT impacts only the eastward extension of the ridge toward the South China Sea, and has a relatively small impact on the upper-level anticyclone over the Tibetan Plateau in both the isolated and full nonlinear response, consistent with their comparatively smaller impact on precipitation. Figure 5e shows the influence of topography on stationary waves when imposed on a basic-state that already includes LSC and OHT, while Figure 5f shows the isolated nonlinear response to topography. The impact of topography is limited to South Asia in the isolated nonlinear response, but is shifted to the west in the full nonlinear response where it contributes to the westward extension of the Asian anti-cyclone. Figure 5g shows the full nonlinear response to LSC, while Figure 5h shows the isolated nonlinear response. Consistent with the lack of a monsoon over South Asia in the isolated nonlinear response, the ridge is confined to East Asia in Figure 5h and does not extend to Western Asia. Similar results are evident for streamfunction at 850 hPa, height at 200 hPa, and zonal wind at 200 hPa (Figures S5–S7).

It is worth noting that the sum of the full nonlinear responses does not equal the stationary waves in CONTROL (not shown), just as the sum of the isolated nonlinear responses does not equal the stationary waves in CONTROL (Figure 5b). Such a lack of additivity is evident for precipitation as well (Figures 2 and 3a).

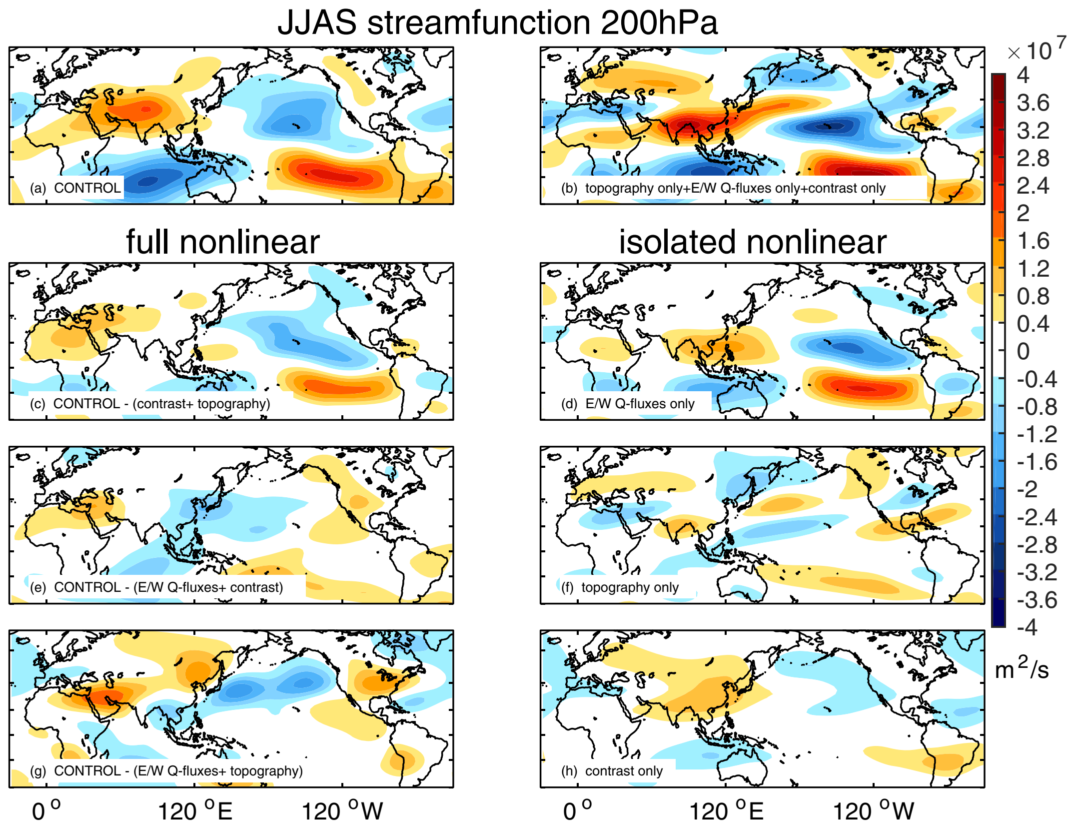

Figure 5. As in Figure 2 but for the deviation of June-September streamfunction at 200 hPa from the zonal average.

Hence it not meaningful to rank the importance of the various building blocks, though both the isolated nonlinear and full nonlinear responses to LSC exceed that in response to topography and OHT at 200 hPa, while at 850 hPa topography and LSC play a similar role (Figure S6).

5. Discussion and Conclusions

Monsoon rainfall is crucial for food security in heavily populated regions of the world. While comprehensive models with realistic land-sea contrast (LSC) and orography simulate these monsoons, it can be difficult to delineate which specific building block in these models is most important for the monsoons. To our knowledge, little work has been done on the possibility of non-additive behavior among these building blocks since the seminal studies of Hoskins and Rodwell (1995) and Rodwell and Hoskins (2001). Simpler models (e.g., moist models with idealized continents) have been used to assess how these individual building blocks lead to monsoons, but these models typically cannot simulate the meridional and zonal structure of observed monsoons. Here, we bridge this gap with a model that can represent the large scale structure of monsoonal precipitation with fidelity, yet allows us to build this monsoonal structure by incrementally adding any or all relevant building blocks (namely LSC, ocean heat transport, and orography) to a zonally symmetric aquaplanet. As discussed in Sections 3 and 4, it is equally instructive to incrementally remove the individual building blocks from a model configuration in which all are initially present. In this way, we do not need to make any a priori assumptions about the relative importance of any specific forcing.

We now summarize the answers to the questions posed in the introduction. The various building blocks of the monsoons interact nonlinearly with each other. Specifically, the response to all three building blocks is considerably weaker if they are added individually to a zonally symmetric aquaplanet, as compared to a configuration in which the other building blocks are already present. This effect is particularly pronounced over South Asia, and less so over East Asia. The question of which forcing is most important is ill-posed in regions with pronounced non-additivity, but generally east-west ocean heat transport is less important over Asia, while topography is less important over West Africa.

This non-additivity can be interpreted in all regions using energetic considerations. In contrast, the land-sea breeze model cannot explain the monsoonal response to LSC. We demonstrate this by considering the surface temperature response to LSC in Figures S8e and S8f. The surface temperature response to LSC is actually larger if LSC is imposed on the no-forcing basic state than when imposed on a basic state that already has the other two forcings (Figures S8e vs. S8f). Only aloft is the temperature response to LSC stronger if LSC is imposed on a basic state that already includes the other forcings (Figures S9e vs. S9f for 200 hPa), consistent with the stronger precipitation and latent heating responses, and these temperature changes are in turn partially responsible for the changes in gross moist stability. Hence, the land-sea breeze model would suggest a stronger monsoon for the isolated nonlinear response to LSC, the opposite of what actually occurs.

Hoskins and Rodwell (1995) and Rodwell and Hoskins (2001) alternately impose orography and heating nominally associated with LSC into a dry model, and reach the conclusion that nonlinearity is small. Namely, the order in which they are imposed has a "slight" impact on the subsequent large scale stationary wave pattern, and they argue that representing diabatic effects explicitly would only positively feed-back on the dry circulation rather than changing its structure. Our results are not in agreement with theirs, as the precipitation and diabatic heating and significantly also the subsequent stationary waves associated with, say, LSC are qualitatively different if LSC is imposed on a background state that includes the other forcings.

The key difference between our studies is that we do not impose a pre-determined diabatic heating, but rather parameterize the underlying processes that influence diabatic heating. In contrast, the diabatic heating imposed by Hoskins and Rodwell is the same regardless of whether orography is present. As discussed in Garfinkel et al. (2020a), diabatic heating is dependent on the flow and thus not independent of orographic forcing (see also Chang, 2009; Held et al., 2002; Nigam et al., 1988), and hence we suggest that Rodwell and Hoskins (2001) underestimate the degree of nonlinearity of the summer stationary wave pattern.

While the model employed here can represent the large scale structure of summer precipitation, it has its limitations. In addition to the simplification to physical processes detailed in Section 2 and Garfinkel et al. (2020b) (e.g., soil moisture, clouds, convection), the east-west transport of heat by the ocean is not coupled to the surface winds, which may lead to an underestimation of their importance (Lutsko et al., 2019). Nevertheless, our key result - there is significant nonlinear interaction among the building blocks - highlights the challenge the monsoonal circulation poses to coupled climate modeling: biases in one component of the model will impact the response ostensibly due to other components, making it challenging to diagnose the source of error. Atmosphere-only model integrations of the "total nonlinear" response, however, can help by providing the fingerprint of biases in each component of the system.

Data Availability Statement

The updated version of MiMA used in this study including the modified source code and example name lists to reproduce the experiments can be downloaded from https://github.com/ianpwhite/MiMA/releases/tag/MiMA-ThermalForcing-v1.0beta (with DOI: https://doi.org/10.5281/zenodo.4523199).

Acknowledgments
CIG, IW, and EPG acknowledge the support of a European Research Council starting grant under the European Union Horizon 2020 research and innovation program (grant agreement number 677756). CIG was also supported by the ISF-NSFC joint research program (grant No.3259/19). EPG also acknowledges support from the US NSF through grant AGS 1852727. MJ acknowledges support from the Australian Research Council (ARC) Centre of Excellence for Climate Extremes (CE170100023) and ARC grant FL 150100035. The authors thank the two anonymous reviewers for their helpful comments. Correspondence should be addressed to C.I.G. (email: chaim.garfinkel@mail.huji.ac.il).

References

Acosta, R., & Huber, M. (2020). Competing topographic mechanisms for the summer indo-asian monsoon. *Geophysical Research Letters*, *47*(3), e2019GL085112. https://doi.org/10.1029/2019gl085112

Baldwin, J. W., Vecchi, G. A., & Bordoni, S. (2019). The direct and ocean-mediated influence of asian orography on tropical precipitation and cyclones. *Climate Dynamics*, *53*(1–2), 805–824. https://doi.org/10.1007/s00382-019-04615-5

Betts, A. K. (1986). A new convective adjustment scheme. part i: Observational and theoretical basis. *Quarterly Journal of the Royal Meteorological Society*, *112*(473), 677–691. https://doi.org/10.1002/qj.49711247307

Betts, A. K., & Miller, M. (1986). A new convective adjustment scheme. part ii: Single column tests using gate wave, bomex, atex and arctic air-mass data sets. *Quarterly Journal of the Royal Meteorological Society*, *112*(473), 693–709. https://doi.org/10.1002/qj.49711247308

Boos, W. R., & Kuang, Z. (2010). Dominant control of the south Asian monsoon by orographic insulation versus plateau heating. *Nature*, *463*(7278), 218–222. https://doi.org/10.1038/nature08707

Bordoni, S., & Schneider, T. (2008). Monsoons as eddy-mediated regime transitions of the tropical overturning circulation. *Nature Geoscience*, *1*(8), 515–519. https://doi.org/10.1038/ngeo248

Chang, E. K. (2009). Diabatic and orographic forcing of northern winter stationary waves and storm tracks. *Journal of Climate*, *22*(3), 670–688. https://doi.org/10.1175/2008jcli2403.1

Chao, W. C., & Chen, B. (2001). The origin of monsoons. *Journal of the Atmospheric Sciences*, *58*, 3497–3507. https://doi.org/10.1175/1520-0469(2001)058h3497:TOOMi2.0.CO;2

Chen, J., & Bordoni, S. (2014). Orographic effects of the Tibetan plateau on the east Asian summer monsoon: An energetic perspective. *Journal of Climate*, *27*(8), 3052–3072. https://doi.org/10.1175/jcli-d-13-00479.1

Chiang, J., Kong, W., Wu, C., & Battisti, D. (2020). Origins of east Asian summer monsoon seasonality. *Journal of Climate*, *33*(18), 7945–7965. https://doi.org/10.1175/jcli-d-19-0888.1

Eltahir, E. A., & Gong, C. (1996). Dynamics of wet and dry years in west Africa. *Journal of Climate*, *9*(5), 1030–1042. https://doi.org/10.1175/1520-0442(1996)009<1030:dowady>2.0.co;2

Frierson, D. M., Held, I. M., & Zurita-Gotor, P. (2006). A gray-radiation aquaplanet moist gcm. part i: Static stability and eddy scale. *Journal of the Atmospheric Sciences*, *63*(10), 2548–2566. https://doi.org/10.1175/JAS3753.1

Frierson, D. M., Held, I. M., & Zurita-Gotor, P. (2007). A gray-radiation aquaplanet moist gcm. part ii: Energy transports in altered climates. *Journal of the Atmospheric Sciences*, *64*(5), 1680–1693. https://doi.org/10.1175/JAS3913.1

Gadgil, S. (2018). The monsoon system: Land–sea breeze or the itcz? *Journal of Earth System Science*, *127*(1), 1. https://doi.org/10.1007/s12040-017-0916-x

Garfinkel, C. I., White, I. P., Gerber, E. P., & Jucker, M. (2020a). The building blocks of northern hemisphere wintertime stationary waves. *Journal of Climate*, *33*(13). https://doi.org/10.1175/JCLI-D-19-0181.1

Garfinkel, C. I., White, I. P., Gerber, E. P., & Jucker, M. (2020b). The impact of sst biases in the tropical east pacific and Agulhas current region on atmospheric stationary waves in the southern hemisphere. *Journal of Climate*, *33*(21), 9351–9374. https://doi.org/10.1175/jcli-d-20-0195.1

Geen, R., Bordoni, S., Battisti, D. S., & Hui, K. (in press). Monsoons, itczs and the concept of the global monsoon. *Reviews of Geophysics*, e2020RG000700. https://doi.org/10.1029/2020RG000700

Geen, R., Lambert, F., & Vallis, G. (2018). Regime change behavior during Asian monsoon onset. *Journal of Climate*, *31*(8), 3327–3348. https://doi.org/10.1175/jcli-d-17-0118.1

Geen, R., Lambert, F. H., & Vallis, G. K. (2019). Processes and timescales in onset and withdrawal of "aquaplanet monsoons". *Journal of the Atmospheric Sciences*, *76*(8), 2357–2373. https://doi.org/10.1175/jas-d-18-0214.1

Gill, A. E. (1980). Some simple solutions for heat-induced tropical circulation. *Quarterly Journal of the Royal Meteorological Society*, *106*, 447–462. https://doi.org/10.1002/qj.49710644905

Halley, E. (1687). An historical account of the trade winds, and monsoons, observable in the seas between and near the tropicks, with an attempt to assign the physical cause of the said winds. *Philosophical Transactions of the Royal Society of London*, *16*(183), 153–168. https://doi.org/10.1098/rstl.1686.0026

Held, I. M., Ting, M., & Wang, H. (2002). Northern winter stationary waves: Theory and modeling. *Journal of Climate*, *15*(16), 2125–2144. https://doi.org/10.1175/1520-0442(2002)015<2125:nwswta>2.0.co;2

Hersbach, H., Bell, B., Berrisford, P., Hirahara, S., Horányi, A., Muñoz Sabater, J., et al. (2020). The era5 global reanalysis. *Quarterly Journal of the Royal Meteorological Society*, *146*(730), 1999–2049. https://doi.org/10.1002/qj.3803

Hoskins, B. J., & Rodwell, M. J. (1995). A model of the Asian summer monsoon. part i: The global scale. *Journal of the Atmospheric Sciences*, *52*(9), 1329–1340. https://doi.org/10.1175/1520-0469(1995)052<1329:amotas>2.0.co;2

Hurley, J. V., & Boos, W. R. (2013). Interannual variability of monsoon precipitation and local subcloud equivalent potential temperature. *Journal of Climate*, *26*(23), 9507–9527. https://doi.org/10.1175/jcli-d-12-00229.1

Iacono, M. J., Mlawer, E. J., Clough, S. A., & Morcrette, J.-J. (2000). Impact of an improved longwave radiation model, rrtm, on the energy budget and thermodynamic properties of the ncar community climate model, ccm3. *Journal of Geophysical Research: Atmospheres*, *105*(D11), 14873–14890. https://doi.org/10.1029/2000jd900091

Jucker, M., & Gerber, E. (2017). Untangling the annual cycle of the tropical tropopause layer with an idealized moist model. *Journal of Climate*, *30*(18), 7339–7358. https://doi.org/10.1175/jcli-d-17-0127.1

Kothawale, D., & Kumar, K. R. (2002). Tropospheric temperature variation over india and links with the indian summer monsoon: 1971-2000. *Mausam*, *53*(3), 289–308.

Li, C., & Yanai, M. (1996). The onset and interannual variability of the asian summer monsoon in relation to land–sea thermal contrast. *Journal of Climate*, *9*(2), 358–375. https://doi.org/10.1175/1520-0442(1996)009<0358:toaivo>2.0.co;2

Lutsko, N. J., Marshall, J., & Green, B. (2019). Modulation of monsoon circulations by cross-equatorial ocean heat transport. *Journal of Climate*, *32*(12), 3471–3485. https://doi.org/10.1175/jcli-d-18-0623.1

Ma, D., Sobel, A. H., Kuang, Z., Singh, M. S., & Nie, J. (2019). A moist entropy budget view of the south asian summer monsoon onset. *Geophysical Research Letters*, *46*(8), 4476–4484. https://doi.org/10.1029/2019gl082089

Maroon, E. A., Frierson, D. M. W., Kang, S. M., & Scheff, J. (2016). The precipitation response to an idealized subtropical continent. *Journal of Climate*, *29*(12), 4543–4564. https://doi.org/10.1175/JCLI-D-15-0616.1

Merlis, T. M., Schneider, T., Bordoni, S., & Eisenman, I. (2013). Hadley circulation response to orbital precession. part ii: Subtropical continent. *Journal of Climate*, *26*(3), 754–771. https://doi.org/10.1175/jcli-d-12-00149.1

Mlawer, E. J., Taubman, S. J., Brown, P. D., Iacono, M. J., & Clough, S. A. (1997). Radiative transfer for inhomogeneous atmospheres: Rrtm, a validated correlated-k model for the longwave. *Journal of Geophysical Research: Atmospheres*, *102*(D14), 16663–16682. https://doi.org/10.1029/97jd00237

Neelin, J. D., & Held, I. M. (1987). Modeling tropical convergence based on the moist static energy budget. *Monthly Weather Review*, *115*(1), 3–12. https://doi.org/10.1175/1520-0493(1987)115<0003:mtcbot>2.0.co;2

Nigam, S., Held, I. M., & Lyons, S. W. (1988). Linear simulation of the stationary eddies in a gcm. part ii: The "mountain" model. *Journal of the Atmospheric Sciences*, *45*(9), 1433–1452. https://doi.org/10.1175/1520-0469(1988)045<1433:lsotse>2.0.co;2

Privé, N. C., & Plumb, R. A. (2007). Monsoon dynamics with interactive forcing. part i: Axisymmetric studies. *Journal of the Atmospheric Sciences*, *64*(5), 1417–1430. https://doi.org/10.1175/jas3916.1

Randel, W. J., & Park, M. (2006). Deep convective influence on the Asian summer monsoon anticyclone and associated tracer variability observed with atmospheric infrared sounder (airs). *Journal of Geophysical Research: Atmospheres*, *111*(D12), D12314. https://doi.org/10.1029/2005jd006490

Raymond, D. J., Sessions, S. L., Sobel, A. H., & Fuchs, Ž. (2009). The mechanics of gross moist stability. *Journal of Advances in Modeling Earth Systems*, *1*(3). https://doi.org/10.3894/james.2009.1.9

Rodwell, M. J., & Hoskins, B. J. (1995). A model of the Asian summer monsoon. part ii: Cross-equatorial flow and pv behavior. *Journal of the Atmospheric Sciences*, *52*(9), 1341–1356. https://doi.org/10.1175/1520-0469(1995)052<1341:amotas>2.0.co;2

Rodwell, M. J., & Hoskins, B. J. (1996). Monsoons and the dynamics of deserts. *Quarterly Journal of the Royal Meteorological Society*, *122*, 1385–1404. https://doi.org/10.1002/qj.49712253408

Rodwell, M. J., & Hoskins, B. J. (2001). Subtropical anticyclones and summer monsoons. *Journal of Climate*, *14*(15), 3192–3210. https://doi.org/10.1175/1520-0442(2001)014<3192:saasm>2.0.co;2

Shaw, T. A. (2014). On the role of planetary-scale waves in the abrupt seasonal transition of the northern hemisphere general circulation. *Journal of the Atmospheric Sciences*, *71*(5), 1724–1746. https://doi.org/10.1175/jas-d-13-0137.1

Simpson, G. (1921). The south-west monsoon. *Quarterly Journal of the Royal Meteorological Society*, *47*(199), 151–171. https://doi.org/10.1002/qj.49704719901

Taylor, K. E. (2001). Summarizing multiple aspects of model performance in a single diagram. *Journal of Geophysical Research: Atmospheres*, *106*(D7), 7183–7192. https://doi.org/10.1029/2000jd900719

Trenberth, K. E., Stepaniak, D. P., & Caron, J. M. (2000). The global monsoon as seen through the divergent atmospheric circulation. *Journal of Climate*. *13*(22), 3969–3993. https://doi.org/10.1175/1520-0442(2000)013<3969:tgmast>2.0.co;2

Vernier, J.-P., Fairlie, T., Natarajan, M., Wienhold, F., Bian, J., Martinsson, B., et al. (2015). Increase in upper tropospheric and lower stratospheric aerosol levels and its potential connection with Asian pollution. *Journal of Geophysical Research: Atmospheres*, *120*(4), 1608–1619. https://doi.org/10.1002/2014jd022372

Wang, B., Ding, Q., & Joseph, P. (2009). Objective definition of the Indian summer monsoon onset. *Journal of Climate*, *22*(12), 3303–3316. https://doi.org/10.1175/2008JCLI2675.1

Wang, P. X., Wang, B., Cheng, H., Fasullo, J., Guo, Z., Kiefer, T., & Liu, Z. (2017). The global monsoon across time scales: Mechanisms and outstanding issues. *Earth-Science Reviews*, *174*, 84–121. https://doi.org/10.1016/j.earscirev.2017.07.006

Wei, H.-H., & Bordoni, S. (2016). On the role of the African topography in the south Asian monsoon. *Journal of the Atmospheric Sciences*, *73*(8), 3197–3212. https://doi.org/10.1175/jas-d-15-0182.1

Wu, G., Liu, Y., He, B., Bao, Q., Duan, A., & Jin, F.-F. (2012). Thermal controls on the asian summer monsoon. *Scientific Reports*, *2*(1), 1–7. https://doi.org/10.1038/srep00404

Xu, Z., Fu, C., & Qian, Y. (2009). Relative roles of land–sea distribution and orography in Asian monsoon intensity. *Journal of the Atmospheric Sciences*, *66*(9), 2714–2729. https://doi.org/10.1175/2009JAS3053.1

Xu, Z., Qian, Y., & Fu, C. (2010). The role of land-sea distribution and orography in the Asian monsoon. part ii: Orography. *Advances in Atmospheric Sciences*, *27*(3), 528–542. https://doi.org/10.1007/s00376-009-9045-z

Zhou, W., & Xie, S.-P. (2018). A hierarchy of idealized monsoons in an intermediate gcm. *Journal of Climate*, *31*(22), 9021–9036. https://doi.org/10.1175/jcli-d-18-0084.1